Spectrochimica Acta Part A 78 (2011) 854–867

Contents lists available at ScienceDirect

Spectrochimica Acta Part A: Molecular and Biomolecular Spectroscopy

journal homepage: www.elsevier.com/locate/saa

Spectroscopic, structure and antimicrobial activity of new Y(III) and Zr(IV) ciprofloxacin

Sadeek A. Sadeek*, Walaa H. El-Shwiniy, Wael A. Zordok, Akram M. El-Didamony

Department of Chemistry, Faculty of Science, Zagazig University, 9 Bab Gamma Street, Zagazig 44519, Egypt

ARTICLE INFO

Article history:
Received 11 April 2010
Received in revised form
11 December 2010
Accepted 14 December 2010

Keywords:
Ciprofloxacin
B3LYP/CEP-31G
Antimicrobial activity

ABSTRACT

The preparation and characterization of the new solid complexes $[Y(CIP)_2(H_2O)_2]Cl_3{\cdot}10H_2O$ and $[ZrO(CIP)_2Cl]Cl{\cdot}15H_2O$ formed in the reaction of ciprofloxacin (CIP) with YCl_3 and $ZrOCl_2{\cdot}8H_2O$ in ethanol and methanol, respectively, at room temperature were reported. The isolated complexes have been characterized with elemental analysis, IR spectroscopy, conductance measurements, UV–vis and ^1H NMR spectroscopic methods and thermal analyses. The results support the formation of the complexes and indicate that ciprofloxacin reacts as a bidentate ligand bound to the metal ion through the pyridone oxygen and one carboxylato oxygen. The activation energies, E^*; entropies, ΔS^*; enthalpies, ΔH^*; Gibbs free energies, ΔG^*, of the thermal decomposition reactions have been derived from thermogravimetric (TGA) and differential thermogravimetric (DTG) curves, using Coats–Redfern and Horowitz–Metzeger methods. The proposed structure of the two complexes was detected by using the density functional theory (DFT) at the B3LYP/CEP-31G level of theory. The ligand as well as their metal complexes was also evaluated for their antibacterial activity against several bacterial species, such as *Staphylococcus aureus* (*S. aureus*), *Escherichia coli* (*E. coli*) and *Pseudomonas aeruginosa* (*P. aeruginosa*) and antifungal screening was studied against two species (*Penicillium* (*P. rotatum*) and *Trichoderma* (*T.* sp.)). This study showed that the metal complexes are more antibacterial as compared to free ligand and no antifungal activity observed for ligand and their complexes.

1. Introduction

Ciprofloxacin (CIP) is a member of the second generation quinolone antibiotics family. It is a broad-spectrum antibiotic that is active against both Gram-positive and Gram-negative bacteria. It functions by inhibiting DNA gyrase, a bacterial type II topoisomerase and topoisomerase IV, which is an enzyme necessary to separate replicated DNA by inhibiting cell division [1].

Quinolones, a commonly used term for the quinolone carboxylic acids or 4-quinolones, are a group of synthetic antibacterial agents containing 4-oxo-1,4-dihydroquinoline skeleton [2]. They can act as antibacterial drugs and the addition of fluorine atom to the original quinolone antibiotic compounds, usually at position 7, yields a new class of drugs, the fluoroquinolones, which have a broader antimicrobial spectrum and improved pharmacokinetic properties [3].

The interactions between metal ions and various quinolones have been reported in the literature [4,5]. These studies have been primarily directed towards the identification of functional groups directly linked to the metal and to establish the structure formed by these coordination complexes. Other investigations aim to show the effect of metal ions upon antibacterial activity [6,7]. The crystal structures of quinolone complexes indicate that quinolone antibiotic can participate in the formation of complexes in a number of ways [8–14]. The neutral ciprofloxacin in the zwitterionic state (Scheme 1) are potentially capable to coordinate with metal ions as a bidentate ligands forming simple complexes via one of the oxygen atoms of the carboxylato group and ring carbonyl group [8,9,12–14].

Infrared spectroscopic and solid state paramagnetic resonance spectroscopy studies of metallic complexes derived from these compounds suggest that they are formed by interaction with the carboxylate group [15]. Density functional theory (DFT) at the B3LYP/CEP-31G level of theory was used to compute the cation type influence on theoretical parameters of the Y(III) and Zr(IV) ciprofloxacin complexes and detect the exact structure of these complexes with different coordination numbers. Such computational characterization reduces time consuming experiments for biomedical and pharmaceutical studies of the drugs and its complexes. Profiles of the optimal set and geometry of these complexes were simulated by applying the GAUSSIAN 98W package of programs [16] at B3LYP/CEP-31G [17] level of theory.

To continue our investigation in the field of quinolone complexes [18–24], we report in the present work, the synthesis and

* Corresponding author. Tel.: +20 0120057510; fax: +0553208213.
E-mail address: sadeek59@yahoo.com (S.A. Sadeek).

1386-1425/$ – see front matter © 2010 Elsevier B.V. All rights reserved.
doi:10.1016/j.saa.2010.12.048

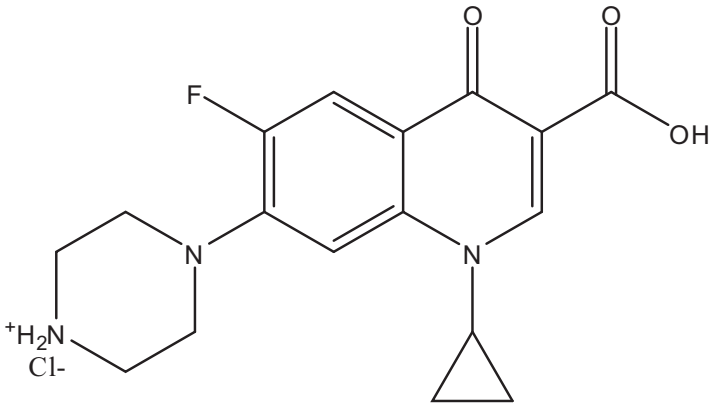

Scheme 1. Structure of ciprofloxacin (CIP) and its zwitterionic state.

characterization of new metal complexes formed from the interaction of CIP with Yttrium(III) and Zirconium(IV) in the solvent and study the effect of oxidation state of the two ions on the biological activity of ciprofloxacin drug. The isolated solid complexes are characterized using spectroscopic and thermal analysis techniques. The thermal behavior of our complexes was studied and the antibacterial activity was tested against several bacterial species, such as *Staphylococcus aureus* (*S. aureus*), *Escherichia coli* (*E. coli*) and *Pseudomonas aeruginosa* (*P. aeruginosa*) and antifungal screening was studied against two species (*Penicillium* (*P. rotatum*) and *Trichoderma* (*T.* sp.)).

2. Materials and methods

2.1. Chemicals

Ciprofloxacin was purchased from Sigma, YCl_3 was purchased from Aldrich Chemical Co., $ZrOCl_2{\cdot}8H_2O$, NaOH and all solvents were purchased from Fluka Chemical Co. All the chemicals and solvents were analytical reagent grade and were used as purchased without further purification.

2.2. Synthesis

An ethanolic solution (20 ml) of ciprofloxacin hydrochloride (1 mmol, 0.3675 g) and NaOH (1 mmol, 0.04 g) was added to an ethanolic solution of YCl_3 (0.5 mmol, 0.0977 g) and the reaction mixture was stirred at room temperature for 48 h. The solution was left for slow evaporation, after that a yellowish-white $[Y(CIP)_2(H_2O)_2]Cl_3{\cdot}10H_2O$ product was deposited. The solid obtained was filtered under vacuum, washed with ethanol and dried. In a similar way, the orange solid complex $[ZrO(CIP)_2Cl]Cl{\cdot}15H_2O$ was prepared by using methanol as a solvent instead of ethanol and using $ZrOCl_2{\cdot}8H_2O$ in 1:2 molar ratio. Unfortunately we were not able to obtained appropriate monocrystals to perform X-ray diffraction analysis. In order to verify that the chloride is ionic and not coordinated, the complex solutions were tested with an aqueous solution of $AgNO_3$ (a precipitate was formed). The two complexes were characterized by their elemental analysis, infrared, electronic, ^{1}H NMR, thermal analysis as well as density functional theory (DFT) at the B3LYP/CEP-31G level of theory.

2.3. Instruments

Elemental C, H, N and halogen analysis was carried out on a Perkin Elmer CHN 2400. The percentage of the metal ions were determined gravimetrically by transforming the solid products into oxide, and also determined by using atomic absorption method. Spectrometer model PYE-UNICAM SP 1900 fitted with the corresponding lamp was used for this purposed. IR spectra were recorded on FTIR 460 PLUS (KBr discs) in the range from 4000 to 400 cm^{-1}, ^{1}H NMR spectra were recorded on Varian Mercury VX-300 NMR Spectrometer using DMSO-d_6 as solvent. TGA-DTG measurements were carried out under N_2 atmosphere within the temperature range from room temperature to 800 °C using TGA-50H Shimadzu. Electronic spectra were obtained using UV-3101PC Shimadzu. Molar conductivities in DMSO at 1.0×10^{-3} M were measured on CONSORT K410.

2.4. Antimicrobial investigation

Antibacterial activity of the complexes/ligand was investigated by a previously reported modified method of Beecher and Wong [25], against different bacterial species, such as *S. aureus*, *E. coli* and *P. aeruginosa* and antifungal screening was studied against two species *P. rotatum* and *Trichoderma* sp. The tested microorganisms isolates were isolated from Egyptian soil and identified according to the standard mycological and bacteriological keys for identification of fungi and bacteria as stock cultures in the microbiology laboratory, Faculty of Science, Zagazig University. The microorganisms were purchased from the laboratory of (Microbiology) in the Faculty of Science, Zagazig University. The nutrient agar medium for antibacterial was (0.5% peptone, 0.1% beef extract, 0.2% yeast extract, 0.5% NaCl and 1.5% agar–agar) and for antifungal (3% sucrose, 0.3% $NaNO_3$, 0.1% K_2HPO_4, 0.05% KCl, 0.001% $FeSO_4$, 2% agar–agar) was prepared and then cooled to 47 °C and seeded with tested microorganisms. After solidification 5 mm diameter holes were punched by a sterile cork-borer. The investigated compounds, ligand and their complexes, were introduced in Petri-dishes (only 0.1 ml) after dissolving in DMSO at 1.0×10^{-3} M. The plates were then incubated for (20 h at 37 °C for bacteria and for 7 days at 30 °C for fungi). At the end of incubation period the inhibition zone around each hole was measured.

3. Results and discussion

The elemental analyses agree well with the proposed structure (Scheme 2) of the two complexes (Table 1). The Y(III) complex is yellowish-white while the Zr(IV) is orange colored complex. They are air stable solids and the higher melting points of the two complexes than ligand revealing that the complexes are much more stable than ligand. The IR spectroscopic and thermogravimetric data confirm the presence of water molecules in the composition of the two complexes. Qualitative reactions revealed the presence of chloride as counter ions in the two complexes. The conductivity

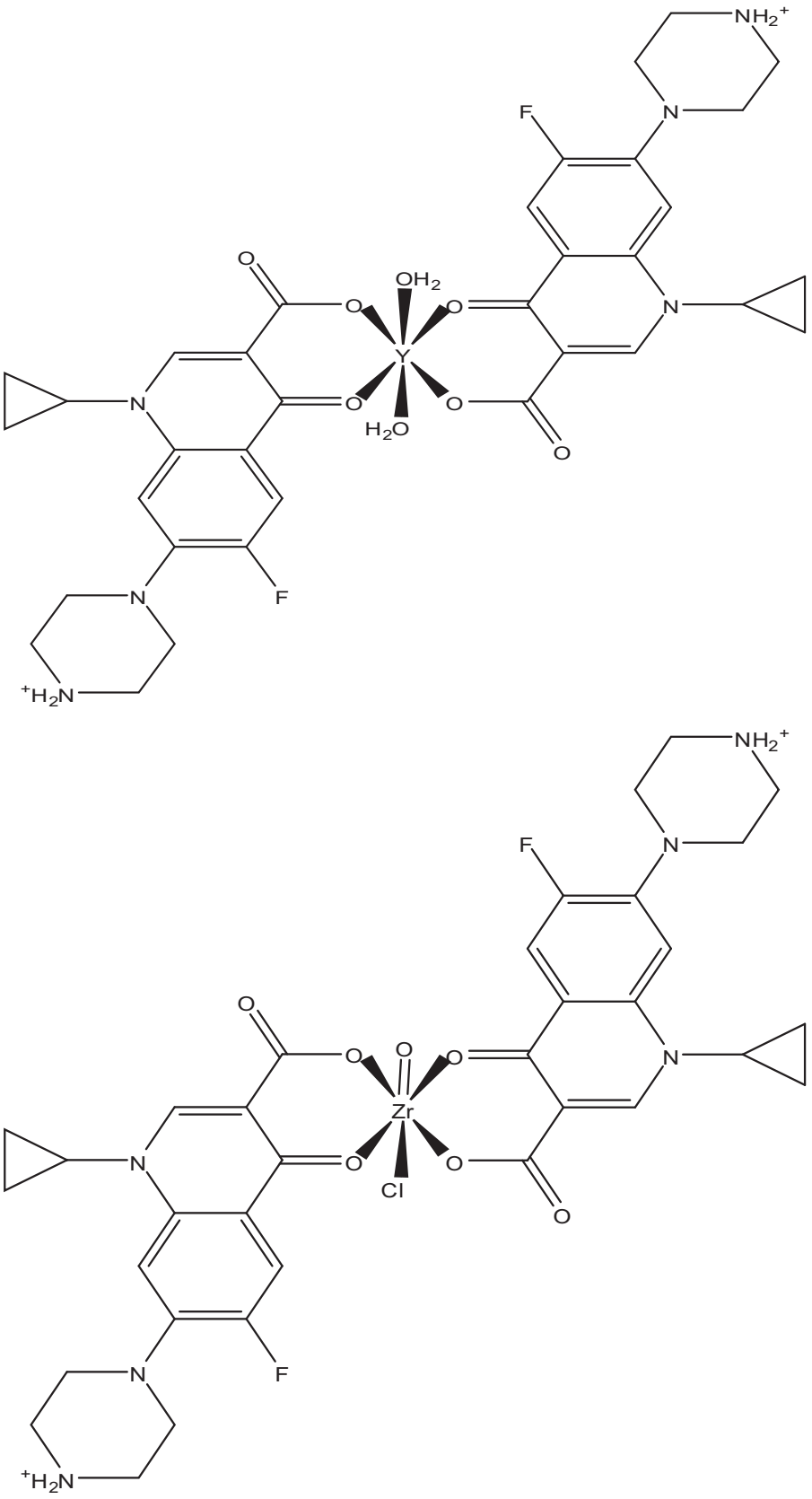

Scheme 2. The coordination mode of Y(III) and Zr(IV) with ciprofloxacin.

Table 1
Elemental analysis and physico-analytical data for the complexes.

Complexes M wt. (M.F.)	Yield (%)	Mp (°C)	Color	Found (calcd.) (%)				
				C	H	N	M	Cl
$[Y(CIP)_2(H_2O)_2]Cl_3{\cdot}10H_2O$ 1073.4 ($C_{34}H_{60}N_6O_{18}F_2Cl_3Y$)	97.79	<360	Yellowish white	(38.01) 37.98	(5.59) 5.53	(7.83) 7.83	(8.28) 8.25	(9.92) 9.90
$[ZrO(CIP)_2Cl]Cl{\cdot}15H_2O$ 1110.22 ($C_{34}H_{66}N_6O_{22}F_2Cl_2Zr$)	49.66	<360	Orange	(36.75) 36.57	(5.95) 5.95	(7.57) 7.47	(8.22) 8.11	(6.40) 6.38

values of Y(III) and Zr(IV) measured in DMSO at room temperature were found at 366.08 and 511.68 S cm^2 mol^{-1}, indicating that the complexes are higher electrolytic nature than ligand [26]. The low conductivity values are in agreement with the low solubility of CIP complexes in water, ethanol, chloroform, acetone and most organic solvents. On the other hand, they are soluble in DMSO, DMF and concentrated acids.

3.1. IR data and bonding

The infrared spectra of the two complexes are compared with those of the free ligand (Table 2), in order to determine the site of coordination that may be involved in chelation. There are some guide peaks in the spectra of the ligand, which are of good help for achieving this goal. These peaks are expected to be involved in chelation. The position or the intensities of these peaks are expected to be changed upon chelation. The presence of the broad bands at 3381 and 3365 cm^{-1} confirms the presence of water molecules in the prepared complexes and the presence of a group of bands with different intensity at 2837, 2818, 2729, 2716, 2508, 2486 and 2362 cm^{-1} (Fig. 1), which assigned to vibration of the quaternized nitrogen of the piperazine group, indicates the zwitterionic form of CIP is involved in the coordination to the metal ions investigated [27]. The two bands observed at 1706 and 1620 cm^{-1} in the spectrum of the free CIP have been assigned to the stretching vibration of carboxylic ν(COOH) and the carbonyl group ν(C=O), respectively, [9,11,18–30].

The disappearance of the band at 1706 cm^{-1} and the shift of the characteristic peak of the carbonyl group ν(C=O) to a lower value from 1620 cm^{-1} to 1577 cm^{-1} for Y(III) and to 1583 cm^{-1} for Zr(IV) indicate coordination of CIP through one of the oxygen atoms of the carboxylato group and of the carbonyl group. The asym-

Table 2
Infrared frequencies (cm^{-1}) and tentative assignments for (A) ciprofloxacin (CIP); (B) $[Y(CIP)_2(H_2O)_2]Cl_3{\cdot}10H_2O$ and (C) $[ZrO(CIP)_2Cl]Cl{\cdot}15H_2O$.

A	B	C	Assignment
3530m	3365m, br	3381m, br	ν(O–H); COOH, H_2O
3381m			
3204vw	3044vw	3046vw	ν(C–H); aromatic
3092m			
3020w			
2925m	2921vw	2932w	ν(C–H); aliphatic
2839m	2837vw	2818vw	
2694ms	2729vw	2716w	
2617ms			
2500w	2508m	2486m	$\nu(-NH_2^+)$
2465ms	2361ms	2362ms	
	2358w	2318w	
1706vs	–	–	ν(C=O); COOH
–	1629vs	1633s	$\nu_{as}(COO^-)$
1620vs	1577ms	1583vw	ν(C=O) and phenyl breathing modes
	1516vw	1520vw	
1455s	1486vs	1481vs	–CH; deformations of $–CH_2$
1390vw	1454vw		
	1410vw		
–	1389vw	1384m	$\nu_s(COO^-)$
1318ms	1346m	1299ms	$\delta_b(–CH_2)$
	1310ms		
1266s	1269vs	1269s	ν(C–O)
1183m	1181ms	1182ms	ν(C–N)
1145m	1112vw	1145ms	ν(C–C)
1104m	1035s	1032s	$\delta_r(–CH_2)$
1026ms	1000w		
987ms	943vw	949s	–CH bend; phenyl
937s	899vw	897s	
835w	839vw	835s	
805w	812m	808m	
754vw	781w	788ms	$\delta_b(COO^-)$
710w	745vw	705vw	
668vw	664w	651vw	ν(M–O) + ring deformation
546ms	622ms	625ms	
478ms	546m	569m	
410s	500m	539m	
		506ms	
		408m	

Keys: s = strong, w = weak, v = very, br = broad, ν = stretching, δ = bending.

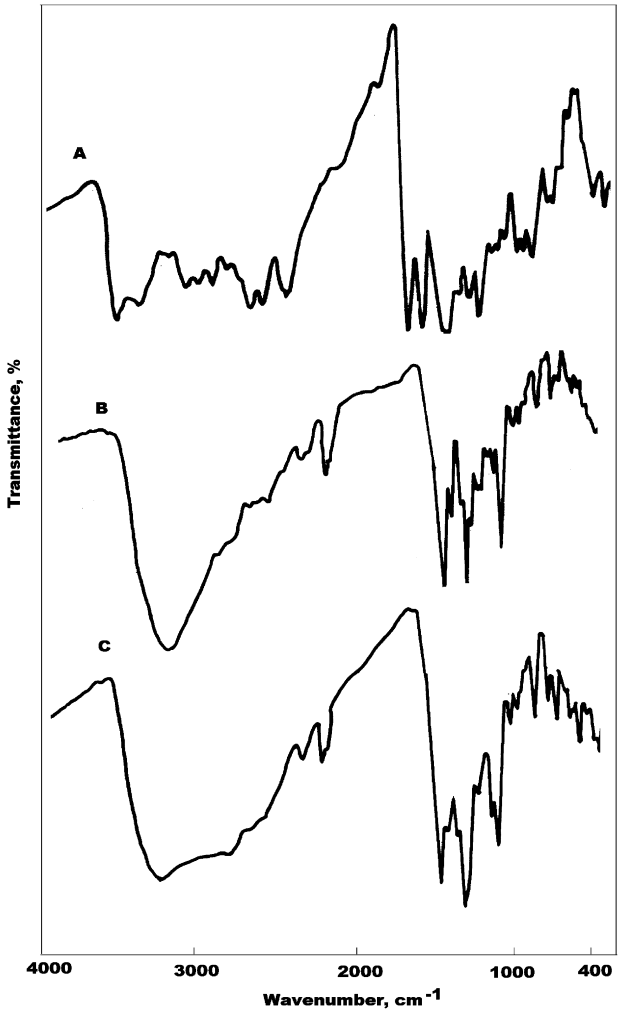

Fig. 1. Infrared spectra of (A) ciprofloxacin (CIP), (B) $[Y(CIP)_2(H_2O)_2]Cl{\cdot}10H_2O$ and (C) $[ZrO(CIP)_2Cl]Cl{\cdot}15H_2O$.

metric stretching vibration (ν_{as}) of the ligated carboxylato group appear at 1629 and 1633 cm^{-1} for Y(III) and Zr(IV) complexes. The spectra of our two complexes also show two bands at 1389 and 1384 cm^{-1}. These bands are absent in the spectrum of CIP and most likely due to the symmetric vibration of the ligated COO^- group. A carboxylate ligand can coordinate to the metal ions either as a monodentate or a bidentate ligand, giving changes in the relative positions of the asymmetric and symmetric stretching vibrations [20–24,30,31]. Unidentate carboxylato complexes exhibit $\Delta\nu$ values > 200 cm^{-1} [$\Delta\nu = \nu_{as}(COO^-) - \nu_s(COO^-)$] [30,31]. The observed $\Delta\nu$ for Y(III) and Zr(IV) CIP complexes are 240 and 249 cm^{-1} suggesting a unidentate interaction of the carboxylato group.

New bands are found in the spectra of the isolated solid complexes with different intensities at 622, 500 cm^{-1} for Y(III) and at 625, 569, 539, 506 cm^{-1} for Zr(IV) (Table 2), which are assigned to ν(M–O) stretching vibrations of coordinated carboxylato oxygen atom and carbonyl oxygen atom. According to the above discussion the CIP is coordinated to metal ions as a bidentate ligand through the oxygen atom of the carboxylato group and the oxygen atom of the carbonyl group.

3.2. UV–vis spectra

The electronic solid reflection spectra of ciprofloxacin along with the Y(III) and Zr(IV) complexes are shown in Fig. 2. The free ciprofloxacin reflected at 243, 298 and 338 nm which attributed to π–π^* and n–π^* intraligand transitions (these transitions occur in case of unsaturated hydrocarbons which contain ketone groups) [31]. The reflection spectra for Y(III) and Zr(IV) ciprofloxacin complexes are practically identical with that of the ligand ciprofloxacin but slightly shifted, indicative of coordination through the pyridone oxygen and one carboxylato oxygen [32]. The two complexes have bands at range from 523 to 576 nm which may be assigned to the ligand to metal charge-transfer [33,34].

3.3. Thermal studies

The ciprofloxacin of Y(III) and Zr(IV) complexes are stable at room temperature and can be stored for several months without any changes. The Y(III) and Zr(IV) ciprofloxacin complexes were studied by thermogravimetric analysis from ambient temperature to 800 °C under a N_2 atmosphere (Fig. 3). The temperature ranges and the percentage mass losses of the decomposition reaction are given in Table 3, together with the evolved moiety and theortical percentage mass losses. The data obtained indicate that the ciprofloxacin is thermally stable in the temperature range 25–50 °C. Decomposition of the CIP starts at 50 °C and finished at 750 °C with two stages. The first stage of decomposition occurs at maximum temperature of 132 °C and is accompanied by a weight loss of 7.81%,

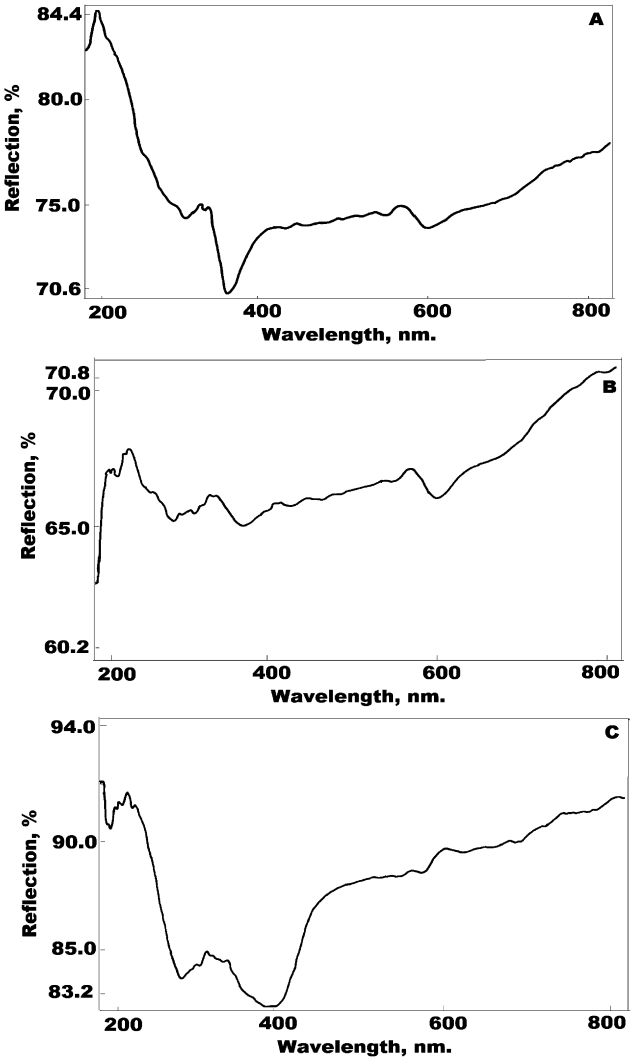

Fig. 2. Electronic reflection spectra of (A) ciprofloxacin (CIP), (B) $[Y(CIP)_2(H_2O)_2]Cl{\cdot}10H_2O$ and (C) $[ZrO(CIP)_2Cl]Cl{\cdot}15H_2O$.

corresponding exactly to the loss of acetylene molecule (C_2H_2). The second stage of decomposition occurs at two maxima 315 and 382 °C and is accompanied by a weight loss of 74.04%, corresponding to the loss of $4C_2H_2 + C_2H_4 + 3NO + HF + 1.5H_2$. The actual weight loss from these stages is equal to 81.85%, very closer to calculated value 81.88%.

The thermal decomposition of $[Y(CIP)_2(H_2O)_2]Cl_3{\cdot}10H_2O$ complex in inert atmosphere proceeds approximately with two

Table 3
The maximum temperature T_{max} (°C)and weight loss values of the decomposition stages for Y(III) and Zr(IV) ciprofloxacins.

Compounds	Decomposition	T_{max} (°C)	Weight loss (%)		Lost species
			Calc.	Found	
CIP ($C_{17}H_{18}N_3O_3F$)	First step	132	7.86	7.81	C_2H_2
	Second step	315, 382	74.02	74.04	$4C_2H_2 + C_2H_4 + 3NO + HF + 1.5H_2$
	Total loss, residue		81.88, 18.12	81.85, 18.15	
$[Y(CIP)_2(H_2O)_2]Cl_3{\cdot}10H_2O$ ($C_{34}H_{60}N_6O_{18}F_2Cl_3Y$)	First step	86	13.415	13.411	$8H_2O$
	Second step	311, 373, 574	70.477	70.476	$10C_2H_2 + 4C_2H_4 + 3HCl + 2HF + CO + 6NO + 1.5H_2O$
	Total loss, residue		83.892, 16.108	83.887, 16.113	
$[ZrO(CIP)_2Cl]Cl{\cdot}15H_2O$ ($C_{34}H_{66}N_6O_{22}F_2Cl_2Zr$)	First step	55	12.970	12.973	$8H_2O$
	Second step	410, 553	67.284	67.276	$10C_2H_4 + 3C_2H_2 + 2HCl + 2HF + 6NO_2$
	Total loss, residue		80.254, 19.746	80.249, 19.751	

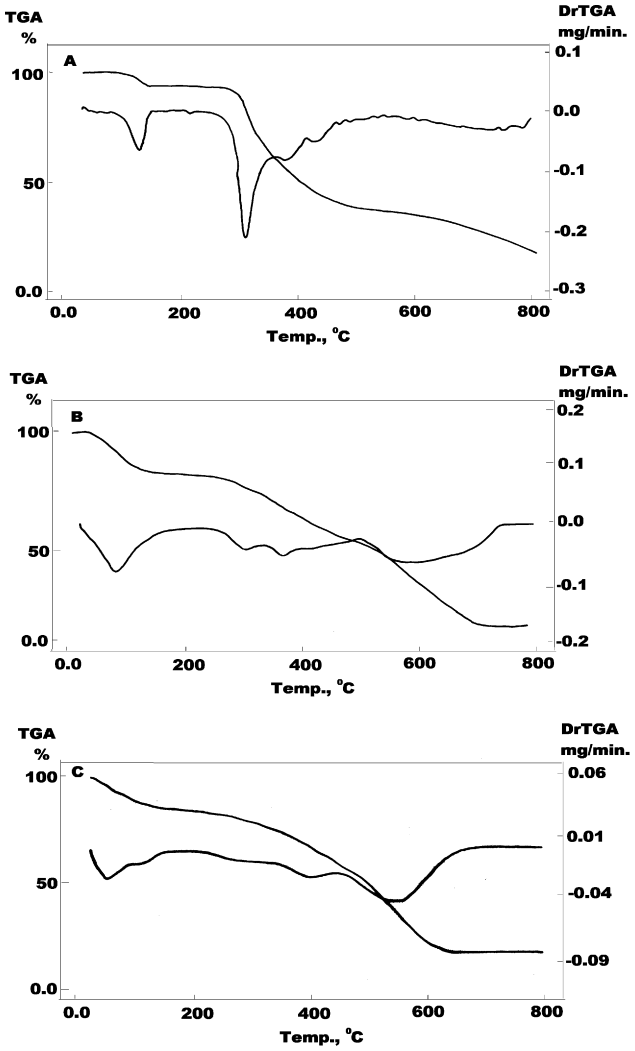

Fig. 3. TGA and DTG diagrams of (A) ciprofloxacin (CIP), (B) $[Y(CIP)_2(H_2O)_2]Cl{\cdot}10H_2O$ and (C) $[ZrO(CIP)_2Cl]Cl{\cdot}15H_2O$.

main degradation steps. The first step of decomposition occurs at maximum temperature of 86 °C and is accompanied by a weight loss of 13.411%, corresponding to the loss of eight water molecules. The second stage of decomposition occurs at maxima temperature of 311, 373 and 574 °C. The weight loss at this step is 70.476%, corresponding to the loss of $10C_2H_2 + 4C_2H_4 + 3HCl + 2HF + CO + 6NO + 1.5H_2O$ as will be described by the mechanism of the decomposition, the final thermal product obtained at 800 °C is $YO_{1.5} + 5C$.

Hydrated Zr(IV) ciprofloxacin complex loss upon heating eight water molecules in the first stage at maximum temperature 55 °C (Table 3). The second step of decomposition occurs at two maxima temperature at 410 and 553 °C. This step is associated with the loss of ciprofloxacin forming $ZrO_2 + 8C$ as a final product. The found weight loss associated with each step of decomposition for our complexes agree well with the calculated weight loss (Table 3). The final products of two complexes obtained at 800 °C were confirmed with infrared spectra.

The proposed structure formula on the basis of the results discussed in this paper located as shown in Scheme 2.

3.4. The kinetics data

Coats and Redfern [35] and Horowitz and Metzger [36] are the two methods mentioned in the literature related to decomposition kinetics studies. The thermodynamic activation parameters of decomposition processes of two complexes namely of $[Y(CIP)_2(H_2O)_2]Cl_3{\cdot}10H_2O$ and $[ZrO(CIP)_2Cl]Cl{\cdot}15H_2O$, the activation energies, E^*; pre-exponential factor, A; entropies, ΔS^*; enthalpies, ΔH^*; Gibbs free energies, ΔG^*, were calculated graphically by employing the Coats Redfern relation. The entropy of activation, ΔS^*, enthalpy of activation, ΔH^* and the free energy change of activation, ΔG^*, were calculated using the following equations:

$$\Delta S^* = 2.303 \left[\log\left(\frac{Ah}{KT}\right)\right] R$$

$$\Delta H* = E* - RT$$

$$\Delta G* = \Delta H* - T\Delta S*$$

The linearization curves of Coats Redfern and Horowitz–Metzger methods are shown in Fig. 4 and all calculations are summarized in Table 4. The entropy of activation was found to have negative values in the two complexes which indicate that the decomposition reactions proceed with a lower rate than normal ones. The correlation coefficients of the Arrhenius plots (r) of the thermal decomposition steps were found to lie in the range

Table 4
Thermal behavior and kinetic parameters determined using the Coats–Redfern (CR) and Horowitz–Metzger (HM) operated for ciprofloxacin and their complexes.

Compounds	Decomposition range (K)	T_s (K)	Method	Parameter					R^a	SD[b]
				$E^* \times 10^4$ (J mol^{-1})	A (s^{-1})	$\Delta S^* \times 10^2$ (J mol^{-1} K^{-1})	$\Delta H^* \times 10^4$ (J mol^{-1})	$\Delta G^* \times 10^5$ (J mol^{-1})		
CIP ($C_{17}H_{18}N_3O_3F$)	323–490	405	CR	8.202	18.08×10^8	−0.7023	7.866	1.0708	0.9575	0.16
			HM	8.112	83.09×10^8	−0.5755	7.776	1.0105	0.9544	0.08
	577–754	588	CR	8.545	1.03×10^6	−1.3544	8.057	1.6015	0.9470	0.21
			HM	8.257	2.97×10^6	−1.2663	7.769	1.5209	0.9349	0.11
$[Y(CIP)_2(H_2O)_2]Cl_3{\cdot}10H_2O$ ($C_{34}H_{60}N_6O_{18}F_2Cl_3Y$)	304–466	359	CR	3.574	3.574×10^4	−1.692	3.275	0.9350	0.9759	0.16
			HM	4.067	1.48×10^5	−1.475	3.768	0.9063	0.9682	0.09
	568–780	584	CR	4.939	0.443×10^3	−1.998	4.454	1.6116	0.9850	0.11
			HM	4.721	0.135×10^4	−1.907	4.236	1.5367	0.9651	0.08
$[ZrO(CIP)_2Cl]Cl{\cdot}15H_2O$ ($C_{34}H_{66}N_6O_{22}F_2Cl_2Zr$)	280–383	328	CR	2.810	2.601×10^3	−1.8032	2.537	0.84513	0.9576	0.17
			HM	3.292	3.292×10^4	−1.5922	3.040	0.8262	0.9493	0.09
	513–683	683	CR	3.763	0.0893×10^3	−2.145	3.195	1.784	0.9872	0.08
			HM	6.413	0.0627×10^5	−1.791	5.845	1.808	0.9975	0.02

[a] Correlation coefficients of the Arrhenius plots.
[b] Standard deviation.

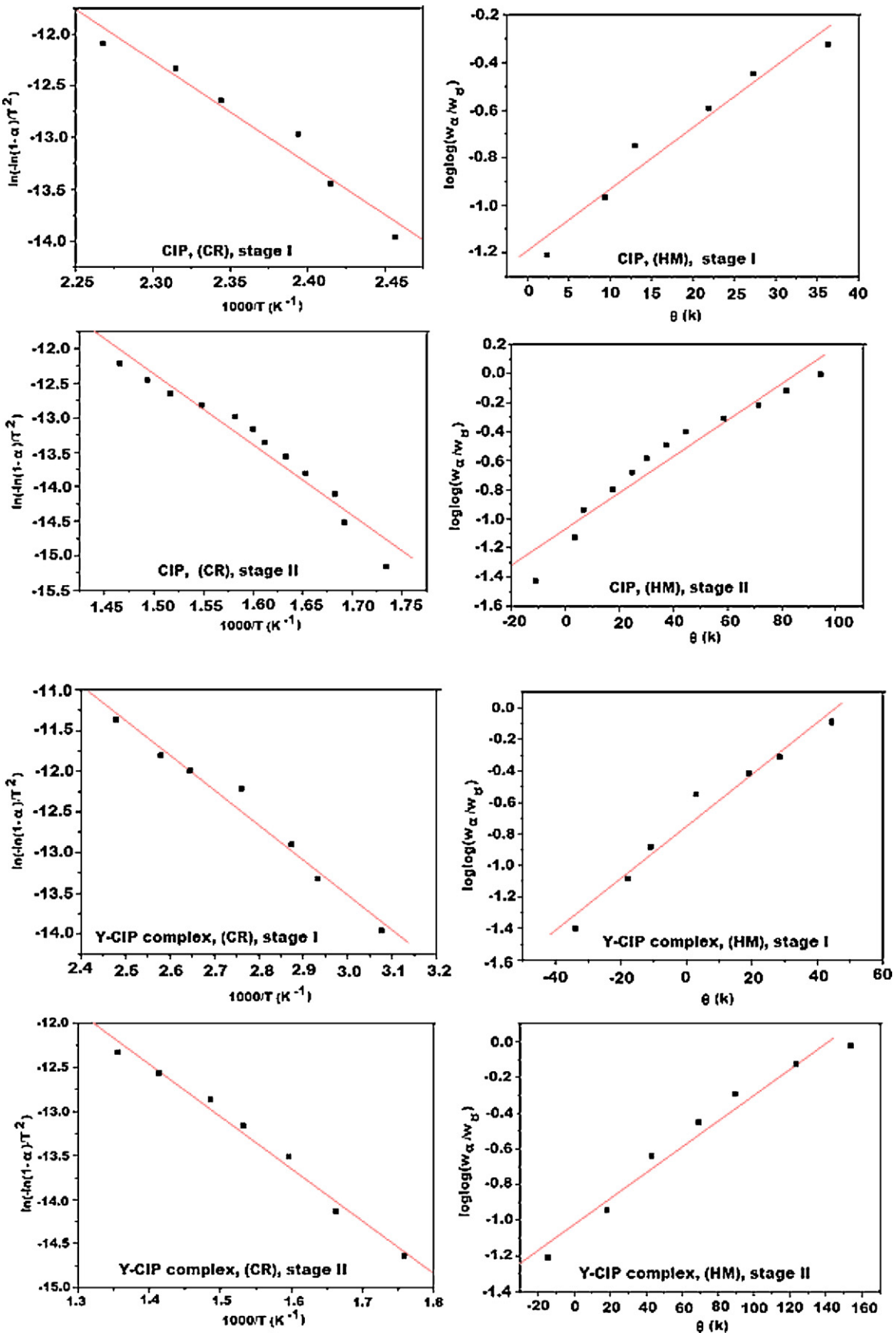

Fig. 4. The diagrams of kinetic parameters of ciprofloxacin; $[Y(CIP)_2(H_2O)_2]Cl{\cdot}10H_2O$ and $[ZrO(CIP)_2Cl]Cl{\cdot}15H_2O$ complexes using Coats–Redfern (CR) and Horowitz–Metzger (HM) equations.

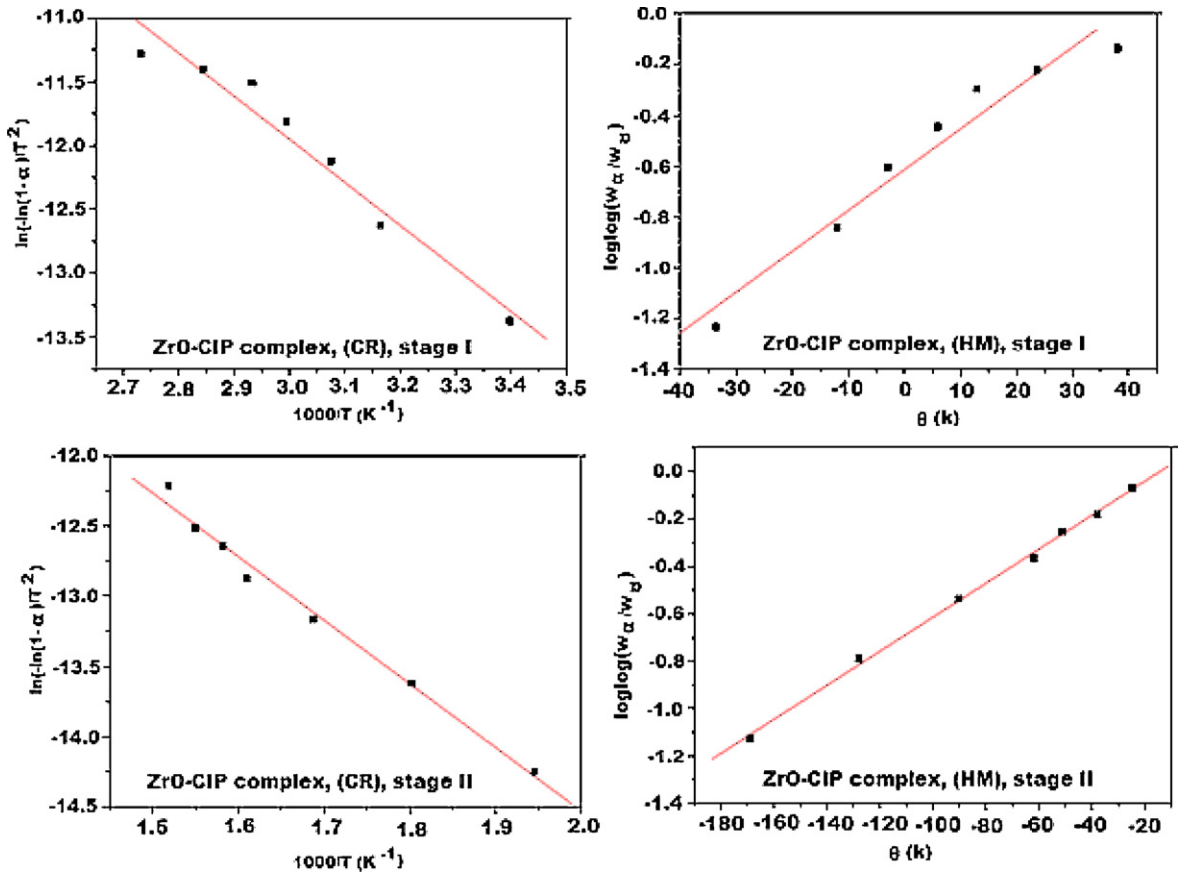

Fig. 4. (*Continued*).

0. 9349–0.9975, showing a good fit with linear function. It is clear that the thermal decomposition process of the two complexes is non-spontaneous, i.e., the complexes are thermally stable.

3.5. The ^1H NMR spectra

The formation of the metal complexes was confirmed by ^1H NMR spectra. Fig. 5 represents the ^1H NMR spectra of $[Y(CIP)_2(H_2O)_2]Cl_3{\cdot}10H_2O$ and $[ZrO(CIP)_2Cl]Cl{\cdot}15H_2O$ complexes which was carried out in DMSO-d_6 as a solvent. Upon comparison with the free ligand, the absent of the characteristic signal for H(COOH) at δ 11.00 ppm in our two complexes indicate coordination of CIP ligand to Y(III) and Zr(IV) through the deprotonated carboxylic group [18–25,37]. The spectra also show characteristic signals for quaternary nitrogen ($-^+NH_2$) at δ 2.484, 2.495 and 2.502 ppm for Y(III) complex and at δ 2.491, 2.497 and 2.502 ppm for Zr(IV) complex. The signal characteristic for water molecules was observed at δ 3.274, 3.340, 3.583, 3.599 and 3.270, 3.330, 3.542, 3.641 ppm for Y(III) and Zr(IV) complexes, respectively, which was not found in the free ciprofloxacin. Also on comparing main signals of ciprofloxacin with its complexes, it is observed that all signals of the free ligand are present in the spectra of the two complexes with chemical shift upon binding of the quinolones to the metal ions [38]. The ^1H NMR data for free CIP and those complexes are summarized in Table 5 and all assignments are given.

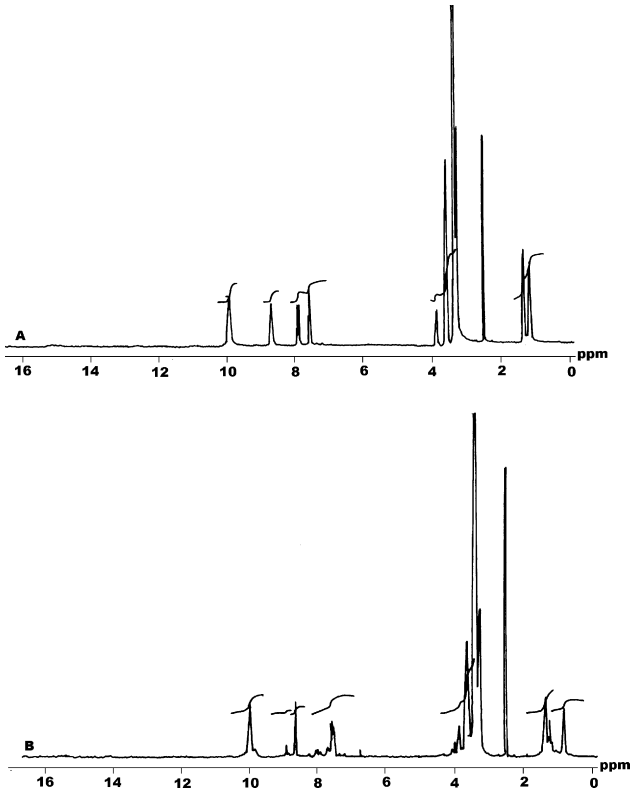

Fig. 5. ^1H NMR spectra of $[Y(CIP)_2(H_2O)_2]Cl{\cdot}10H_2O$ and $[ZrO(CIP)_2Cl]Cl{\cdot}15H_2O$ complexes in DMSO, δ_{TMS}.

3.6. Biological activities test

The susceptibility of certain strains of bacterium, such as *S. aureus*, *E. coli* and *P. aeruginosa* and antifungal screening was studied against two species *P. rotatum* and *Trichoderma* sp. towards

Table 5
^{1}H NMR values (ppm) and tentative assignments for (A) ciprofloxacin (CIP); (B) $[Y(CIP)_2(H_2O)_2]Cl_3{\cdot}10H_2O$ and (C) $[ZrO(CIP)_2Cl]Cl{\cdot}15H_2O$.

A	B	C	Assignments
1.33	1.157, 1.222, 1.249, 1.273	0.818, 1.040, 1.221, 1.260, 1.358	δ H, $-CH_3$
2.00	–	–	δ H, –NH; piperazine
–	2.484, 2.495, 2.502	2.491, 2.497, 2.502	δ H, $-^+NH_2$
–	3.274, 3.340, 3.583, 3.599	3.270, 3.330, 3.542, 3.641	δ H, H_2O
2.78, 3.46	3.873	3.877, 3.991, 4.069	δ H, $-CH_2$ aliphatic
6.04, 8.01, 8.66	7.589, 7.614, 7.910,8.704	6.763, 7.511, 7.957, 8.654	δ H, $-CH_2$ aromatic
11.00	–	–	δ H, –COOH

Table 6
The inhibition diameter zone values (mm) for CIP and their complexes.

Compounds	Microbial species				
	Bacteria			Fungi	
	Escherichia coli	*Pseudomonas aeruginosa*	*Staphylococcus aureus*	*Penicillium rotatum*	*Trichoderma* sp.
CIP	27 ± 0.3464	23 ± 0.1155	26 ± 0.4041	0	0
Y(III)/CIP	29^{+1} ± 0.4450	25^{+1} ± 0.4041	36^{+3} ± 0.1472	0	0
Zr (IV)/CIP	29.5^{+1} ± 0.3227	34^{+2} ± 0.2540	37^{+3} ± 0.3868	0	0
Control (DMSO)	0	0	0	0	0

Statistical significance $P^{(NS)}P$ not significant, $P > 0.05$; $P^{(+1)}P$ significant, $P < 0.05$; $P^{(+2)}P$ highly significant, $P < 0.01$; $P^{(+3)}P$ very highly significant, $P < 0.001$; Student's *t*-test.

ciprofloxacin and its complexes was judged by measuring size of the inhibition diameter. As assessed by color, the complexes remain intact during biological testing (Table 6, Fig. 6). A comparative study of ligand and their metal complexes showed that the metal complexes exhibit higher antibacterial activity for Gram-positive one *S. aureus* and Zr(IV) is more effective antibacterial for *P. aeruginosa* than *E. coli* Gram-negative but Y(III) showed moderated antibacterial activity for *E. coli* and *P. aeruginosa* (Table 6), and no antifungal activity observed for ligand and their metal complexes. The results are promising compared with the previous studies [39–41]. Such increased activity of metal chelate can be explained on the basis of the oxidation state of the metal ion, overtone concept and chelation theory. According to the overtone concept of cell permeability, the lipid membrane that surrounds the cell favors the passage of only lipid-soluble materials in which liposolubility is an important factor that controls the antimicrobial activity. On chelation the polarity of the metal ion will be reduced to a greater extent due to overlap of ligand orbital and partial sharing of the positive charge of the metal ion with donor groups. Further it increases the delocalization of π-electrons over the whole chelate ring and enhances the lipophilicity of the complexes [40]. This increased lipophilicity enhances the penetration of complexes into the lipid membranes and blocks the metal binding sites in enzymes of microorganisms. These complexes also disturb the respiration process of the cell and thus block the synthesis of proteins, which restricts further growth of the microorganisms. We also found that the increasing of oxidation state of the metal ion increasing the antibacterial activity of ciprofloxacin drug. Also, the Y(III) and Zr(IV) ions are increasing the solubility of ciprofloxacin, this increase of hydrophilicity can enhance the ability of drug molecules in crossing the membrane of a cell, and hence raise the biological utilization ratio and activity of the drug. The differences between the free ciprofloxacin ligand and the two complexes are statistically significant, the Δ values are lying down in the error-range of the method and the statistical treatment of the results is clearly specified as shown in Table 6 and Fig. 6.

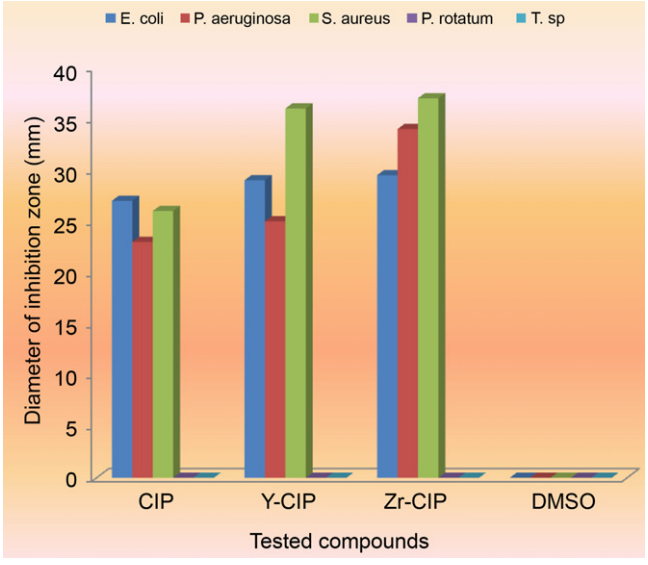

Fig. 6. Statistical representation for biological activity of ciprofloxacin acid and its metal complexes.

3.7. Computational details

Computational method used: the computer used in theoretical studies was a CPU: AMD A Thlon XP 2.4 GHz, Ram 512 DDR/333 MHz; Cache: 512 K. The geometrical optimization was carried out at DFT level of theory using the Gaussian 98W package of programs [16]. The DFT methods compute electron correlation via general functionals of the electron density. The calculations carried out at B3LYP/CEP-31G level of theory [17]. The basis set CEP-31G is more accurate for the studying of the d-block elements. This high basis set has been chosen to detect the dipole moment at a very accurate level.

3.7.1. Computational method

The geometric parameters and energies were computed by density functional theory (DFT) at the B3LYP/CEP-31G level of theory, using the GAUSSIAN 98W package of the programs, on geometries that were optimized at CEP-31G basis set. The high basis set was chosen to detect the energies at a highly accurate level. The atomic charges were computed using the natural atomic orbital populations. The B3LYP is the key word for the hybrid functional [42], which is a linear combination of the gradient functionals proposed by Becke [43] and Lee et al. [44], together with the Hartree–Fock local exchange function [45].

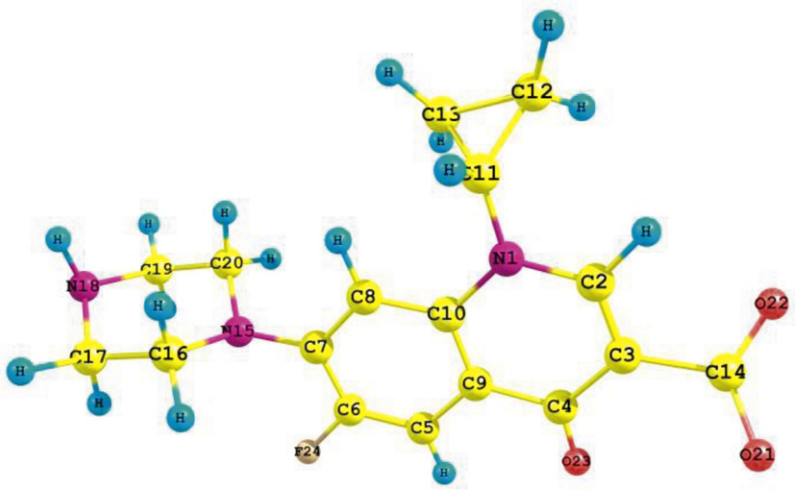

Scheme 3. The optimized geometrical of ciprofloxacin by using B3LYP/CEP-31G.

3.7.2. Structural parameters and models

3.7.2.1. Ciprofloxacin. A role of the quinolone molecule in the structure is similar to the ionic compounds reported [9,11,46], it is protonated at a terminal nitrogen atom of piperazine ring N18. The bond lengths for C4–O23, C14–O22 and C14–O21 are 1.28, 1.26 and 1.29 Å, respectively [47]. Detailed analysis of corresponding bond lengths in various quinolone molecules was given elsewhere [29]. All these distances as well as the angles between the atoms of the rigid quinolone ring system and those of the piperazine ring are similar appearance described earlier [9,11,46].

The biological activity of quinolones (ciprofloxacin) is mainly determined by its fine structure, the ciprofloxacin has many characteristic structural features. The molecule is a highly sterically hindered, the cyclopropyl ring not located in the same plane of quinolone ring with the dihedral angles C10–N1–C11–C13 and C10–N1–C11–C12 are −73.47 and −143.95, also the piperazine group out of plane of the molecule. This observation is supported by the values of calculated dihedral angles: C20–N15–C7–C8, 65.70 and C16–N15–C7–C8, −69.70, where the values are neither zero nor 180. Scheme 3 shows the optimized geometrical of ciprofloxacin molecule, the dihedral angles O23–C4–C3–C14, O21–C14–C3–C4 and O22–C14–C3–C4 are 0.00, −38.5 and 145.45 which confirms that the O23 and O21 located in the same direction. The plane of C4–O23 bond located in the same plane of C14–O21 bond while O23 and O22 are located in the opposite direction to each other so, the plane of C4–O23 is not found in the same plane of C14–O22.

Table 7 gives the optimized geometry of ciprofloxacin as obtained from B3LYP/CEP-31G calculations. These data are drawing to give the optimized geometry of molecule. The value of bond angle C4–C3–C14 is 123.67 which reflects a sp^2 hybridization of C8, the same result is obtained with C4 and C14. These values of bond distances agree well with the previously reported values for similar ciprofloxacinate complexes [47,29,48–50].

Charge distribution on the optimized geometry of ciprofloxacin is given in Table 7. There is a significant built up of charge density on the oxygen atoms which is distributed over all molecule, the charge on O21 of carboxylate group is −0.356 and O23 of ketone group is −0.133, so ciprofloxacin molecule behaves as bidentate ligand (O_{keto} and $O_{carboxylate}$ atoms) and the molecule is a highly dipole μ = 24.5 D.

3.7.2.2. The Y(III) ciprofloxacin complexes. The Y(III) chelated with two ciprofloxacin molecules through four oxygen atoms (O_{keto} and $O_{carboxylate}$ atoms) forming four coordinate bonds. The experimental data shows set that the result complex is six-coordinate so, the complex consists of four coordinate bonds with two ciprofloxacin molecules and the other two coordinate bonds may be water molecules or chloride ions. In this part we study theoretically the proposed two structures of $[Y(CIP)_2Cl_2]^+$ and $[Y(CIP)_2(H_2O)_2]^{+3}$.

3.7.2.2.1. Description of the structure of $[Y(CIP)_2Cl_2]^+$. Scheme 4 shows the optimized geometrical of the complex with the atomic numbering schema. The selected bond distances and angles are given in Table 8 and the suggested complex is composed of $[Y(CIP)_2Cl_2]^+$, where the Y(III) ion is in a distorted octahedral environment. In the axial plane the metal ion is coordinated by four oxygen atoms (O_{keto} and $O_{carboxylate}$) of two ciprofloxacin ligands at the distances vary from 2.229 Å to 2.237 Å, these bond lengths are similar to those observed in related compounds [48]. The difference in the bond length for the carboxylate O21a–C14a and O22a–C14a (1.350 Å and 1.212 Å) [49], confirms the formation of bond between the ionic carboxylate oxygen atom and Y(III) ion. The octahedral coordination environment is completed by two chloride ions. The bond distances between Y–O21a and Y–O23a are 2.229

Table 7
Equilibrium geometric parameters bond lengths (Å), bond angles (°), dihedral angles (°) and charge density of ciprofloxacin ligand by using DFT/B3LYP/CEP-31G.

Bond length (Å)			
C4–O23	1.28 (1.30) [47]	C3–C14	1.51 (1.47) [47]
C4–C3	1.47 (1.41)	C14–O22	1.26 (1.23)
C2–C3	1.38 (1.38)	C14–O21	1.29 (1.29)
C10–N1	1.41 (1.40)	C11–N1	1.46 (1.46)
Bond angle (°)			
C7–N15–C20	115.08	O23–C4–C3	124.89
C7–N15–C16	114.66	O21–C14–C3	114.95
N15–C7–C8	121.97	O22–C14–C3	114.92
N15–C7–C6	120.17	O21–C14–O22	129.98
C4–C3–C14	123.67	C2–N1–C11	120.36
Dihedral angles (°)			
O23–C4–C3–C2	177.90	C10–N1–C11–C13	−73.47
C16–N15–C7–C8	−69.70	C11–N1–C2–C3	177.40
C20–N15–C7–C8	65.70	O23–C4–C3–C14	0.00
C10–N1–C11–C12	−143.95	O22–C14–C3–C4	145.45
	O21–C14–C3–C4	−38.5	
Charges			
N1	0.178	O23	−0.133
N15	−0.098	O21	−0.356
N18	−0.279	O22	−0.369
C14	−0.018	C2	−0.305
C4	−0.386	C3	0.187
Total energy/au	−207.81236		
Total dipole moment/D	24.5		

( ): Ref. [47].

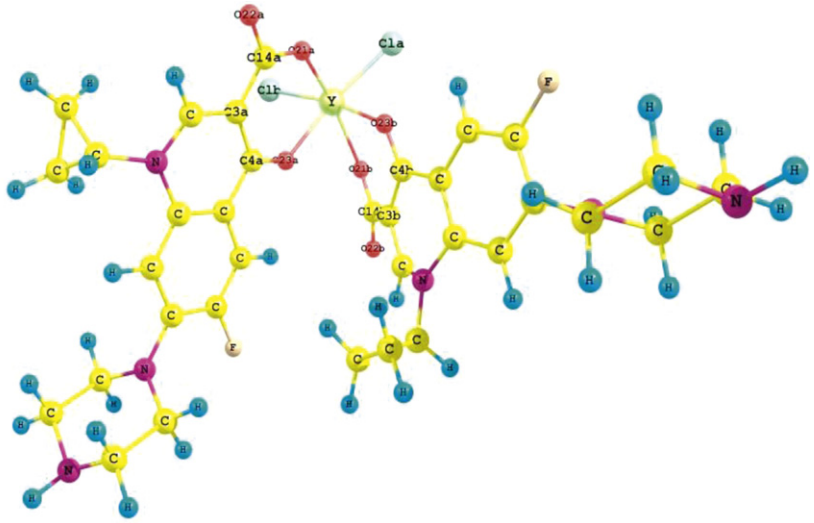

Scheme 4. Optimized geometrical of $[Y(CIP)_2Cl_2]^+$ complex by using B3LYP/CEP-31G.

and 2.234 Å [50] while the distance between Y–Cl is 2.611 Å [51]. The bond lengths of Y–O23a and Y–O23b are 2.234 and 2.237 Å which are longer than that of Y–O21a and Y–O21b (2.229 Å and 2.231 Å). Both are similar to these observed in related quinolone Y(III) compounds [50]. The bond angles around the central metal ion Y(III) vary from 78.41 to 100.32; these values differ significantly from these expected for a distorted octahedron.

It is important to note that, in the complex, the C14a–O21a and C4a–O23a bond lengths become equal 1.350 and 1.289 Å, respectively, and slightly longer than those found in free ligand of ciprofloxacin (1.290 and 1.280 Å, respectively). The energy of this complex is −483.919 au and the dipole moment is weak 4.601 D, so this complex is less stable.

3.7.2.2.2. Description of the structure of $[Y(CIP)_2(H_2O)_2]^{+3}$. Table 9 lists selected inter atomic distances and angles. The structure of complex with atomic numbering schema is shown in Scheme 5. The complex consists of two units of ciprofloxacin molecule and two water molecules with Y(III) metal ion. The complex is six-coordinate with distorted octahedral environment around the metal ion. The Y(III) metal ion is coordinated to one O_{keto} atom and $O_{carboxylate}$ atom of ciprofloxacin ligand and two O_{H_2O} atoms for water. The bond distances between Y–O21a and Y–O23a are 2.221 and 2.222 Å, while the distance between Y–O_{H_2O} is 2.44 Å [50]. Also the angles around the central Y(III) metal ion with surrounding oxygen atoms vary from 78.84 to 122.70; these values differ legally from these expected for a distorted octahedron. The distances and angles in the quinolone ring system, as well as those of piprazine rings are similar to those found in reported structure of free ciprofloxacin [50].

The bond distances between Y(III) and surrounded oxygen atoms of ciprofloxacin in water complex are shorter than that in chloride complex as shown in Tables 8 and 9, so that the Y(III) metal ion is bonded strongly with surrounded oxygen atoms of ciprofloxacin in water complex more than that in chloride complex. Also the charges accumulated on $O_{carboxylate}$ are −0.307 and −0.276 and for O_{keto} are −0.183 and −0.242 for water complex while for the chloride complex the charges on $O_{carboxylate}$ are −0.304 and −0.299 and for O_{keto} are 0.041 and 0.037. There is a strong inter-

Table 8
Equilibrium geometric parameters bond lengths (Å), bond angles (°) and charge density of $[Y(CIP)_2Cl_2]^+$ by using DFT/B3LYP/CEP-31G.

Bond length (Å)			
Y–O21a	2.229 [50]	C4b–O23b	1.289 [49]
Y–O23a	2.234 [50]	C14b–O21b	1.348 [49]
Y–O21b	2.231 [50]	C14a–O21a	1.350 [49]
Y–O23b	2.237 [50]	C4a–O23a	1.289 [49]
Y–Cla	2.611 [51]	C14a–O22a	1.212 [49]
Y–Clb	2.610 [51]	C14b–O22b	1.212 [49]
Bond angle (°)			
O21a–Y–O23a	81.87 [48]	O21b–Y–O23a	78.41 [48]
O21a–Y–O23b	79.11 [48]	O21a–Y–Clb	97.86
O21a–Y–Cla	99.73	O23a–Y–Clb	88.10
O21b–Y–Clb	100.32	O21b–Y–Cla	97.19
O21b–Y–O23b	79.04 [48]	Cla–Y–Clb	99.82
O23b–Y–Cla	91.46		
Charges			
Y	0.89	Cla	−0.452
O23a	0.041	Clb	−0.449
O21a	−0.304	O23b	0.037
O22a	−0.058	O21b	−0.299
O22b	−0.058		
Total energy/au		−483.919	
Total dipole moment/D		4.601	

Table 9
Equilibrium geometric parameters bond lengths (Å), bond angles (°) and charge density of $[Y(ClP)_2H_2O]^{+3}$ by using DFT/B3LYP/CEP-31G.

Bond length (Å)			
Y–O21a	2.221 [50]	C14b–O22b	1.264 [49]
Y–O23a	2.222 [50]	C14b–O21b	1.322 [49]
Y–O21b	2.333 [50]	C4a–O23a	1.296 [49]
Y–O23b	2.181 [50]	C14a–O22a	1.261 [49]
Y–Oa	2.400 [50]	C14a–O21a	1.323 [49]
Y–Ob	2.440 [50]	C4b–O23b	1.298 [49]
Y–O_{H_2O}	2.44 Å [48]		
Bond angle (°)			
O21b–Y–O23b	82.86 [48]	O21a–Y–O23b	122.70 [48]
O21b–Y–O23a	81.64 [48]	O21a–Y–Oa	101.86
O21b–Y–Oa	81.65	O21a–Y–Ob	81.32
O21b–Y–Ob	78.84	O23a–Y–Oa	80.97
O21a–Y–O23a	86.93 [48]	O23a–Y–Ob	81.23
O23b–Y–Oa	82.96	Oa–Y–Ob	80.36
Charges			
Y	1.173	Oa	0.219
O23a	−0.183	Ob	0.217
O21a	−0.307	O23b	−0.242
O22a	−0.095	O21b	−0.276
O22b	−0.112	C14a	−0.529
C14b	−0.514		
Total energy/au		−487.9834	
Total dipole moment/D		36.85	

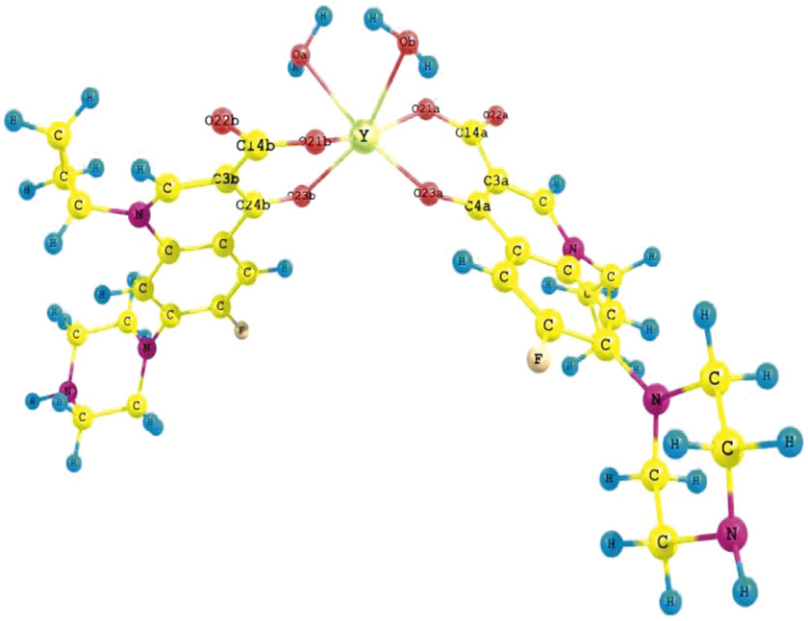

Scheme 5. Optimized geometrical of $[Y(ClP)_2(H_2O)_2]^{+3}$ complex by using B3LYP/CEP-31G.

action between central Y(III) metal ion which has become charge equal +1.173 and more negative oxygen atoms in water complex greater than that in chloride complex, at which Y(III) becomes has less positively charge (+0.89) in chloride complex. The energy of this complex is −487.9834 au and highly dipole 36.85 D. For all these reasons the water complex is more stable than chloride complex and Y(III) favor coordinated with two water molecules more than two chloride ions to complete the octahedron structure.

3.7.2.3. The Zr(IV) ciprofloxacin complexes. The Zr(IV) may be chelated with two molecules of ciprofloxacin through four oxygen atoms forming four coordinate bonds (O_{keto} and $O_{carboxylate}$). The experimental data set that the result complex is six-coordinate so, the complex consists of four coordinate bonds with two ciprofloxacin molecules and one coordinated bond may be with water molecule or chloride ion beside oxygen atom of ZrO ion. In this part we study theoretically the all possible structures can be obtained $[ZrO(ClP)_2Cl]^+$ and $[ZrO(ClP)_2H_2O]^{+2}$.

3.7.2.3.1. Description of the structure $[ZrO(ClP)_2H_2O]^{+2}$. Table 10 lists selected inter atomic distances and angles. The structure of complex with atomic numbering schema is shown in Scheme 6. The complex consists of two units of ciprofloxacin molecule and one water molecule with Zr(IV) ion of ZrO unit. The complex is six-coordinate with distorted octahedral environment around the metal ion. The Zr(IV) metal ion is coordinated to one O_{keto} atom and one $O_{carboxylate}$ atom of ciprofloxacin ligand and O_{H_2O} atom for water. The Zr–O21a and Zr–O21b bond lengths are 2.063 and 2.062 Å, which are shorter than that of Zr–O23a

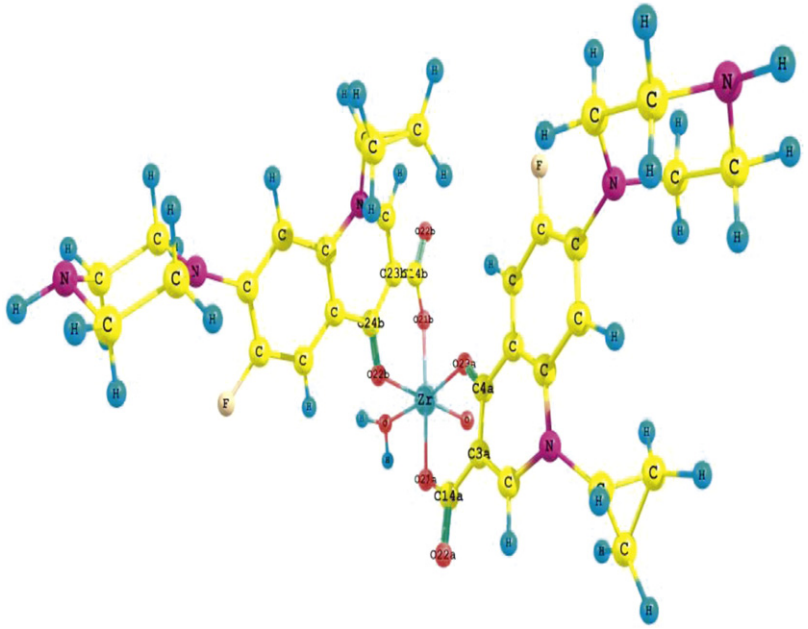

Scheme 6. Optimized geometrical of $[ZrO(ClP)_2H_2O]^{+2}$ complex by using B3LYP/CEP-31G.

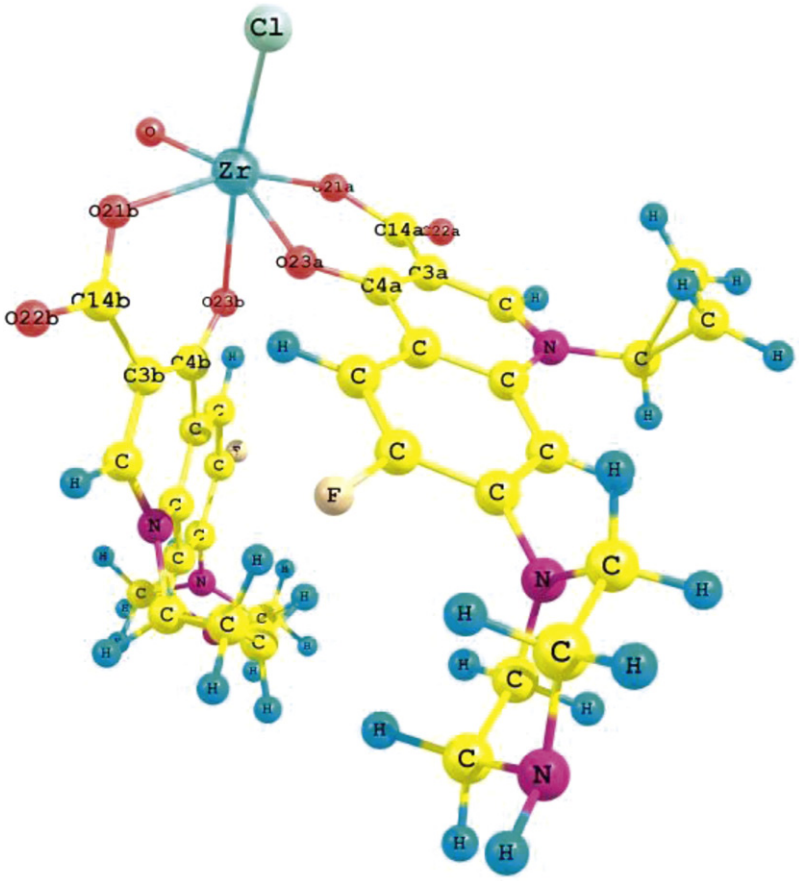

Scheme 7. Optimized geometrical of $[ZrO(CIP)_2Cl]^+$ complex by using B3LYP/CEP-31G.

and Zr–O23b (2.070 and 2.067 Å) and the bond distance between Zr–O_{H_2O} is 2.114 Å [52]. Also the angles around the central Zr(IV) metal ion with surrounding oxygen atoms vary from 82.57 to 95.41; these values not differ legally from these expected for a distorted octahedron. The energy of this complex is −494.170173 au while the dipole moment is weak 5.821 D, so this complex is less stable.

3.7.2.3.2. Description of the structure of $[ZrO(CIP)_2Cl]^+$. Table 11 lists selected inter atomic distances and angles. The structure of complex with atomic numbering schema is shown in Scheme 7. The complex consists of two units of ciprofloxacin molecule and one chloride ion with Zr(IV) ion in ZrO. The complex is six-coordinate with distorted octahedral environment around the metal ion. The Zr(IV) metal ion of ZrO is coordinated to one O_{keto} atom and

Table 10
Equilibrium geometric parameters bond lengths (Å), bond angles (°) and charge density of $[ZrO(CIP)_2H_2O]^{+2}$ by using DFT/B3LYP/CEP-31G.

Bond length (Å)			
Zr–O21a	2.063 [54]	C14b–O22b	1.211
Zr–O23a	2.070 [55]	C14b–O21b	1.349
Zr–O21b	2.062 [54]	C4a–O23a	1.212
Zr–O23b	2.067 [55]	C14a–O22a	1.211
Zr–O	2.112	C14a–O21a	1.349
Zr–O_{H_2O}	2.114	C4b–O23b	1.210
Bond angle (°)			
O21b–Zr–O23b	87.53 [56]	O21a–Zr–O23b	82.57
O21b–Zr–O23a	84.34 [56]	O21a–ZrO	94.86
O21b–ZrO	95.41	O21a–Zr–O_{H_2O}	93.28
O21b–Zr–O_{H_2O}	95.15	O_{H_2O}–ZrO	93.96
O21a–Zr–O23a	85.09	O23a–Zr–O_{H_2O}	87.93
O23b–ZrO	94.27	O23b–Zr–O23a	83.85
Charges			
Zr	0.829	O	0.158
O23a	−0.335	O_{H_2O}	−0.279
O21a	−0.367	O23b	−0.376
O22a	−0.374	O21b	−0.372
O22b	−0.376		
Total energy/au		−494.170173	
Total dipole moment/D		5.821	

Table 11
Equilibrium geometric parameters bond lengths (Å), bond angles (°) and charge density of $[ZrO(CIP)_2Cl]^+$ by using DFT/B3LYP/CEP-31G.

Bond length (Å)			
Zr–O21a	2.192 [54]	C14b–O22b	1.284
Zr–O23a	2.404 [55]	C14b–O21b	1.359
Zr–O21b	2.194 [54]	C4a–O23a	1.308
Zr–O23b	2.195 [55]	C14a–O22a	1.287
Zr–O	2.430	C14a–O21a	1.362
Zr–Cl	2.299 [52,53]	C4b–O23b	1.322
Bond angle (°)			
O21b–Zr–O23b	93.06 [56]	O21a–Zr–O23b	79.38
O21b–Zr–O23a	73.05 [56]	O21a–ZrO	90.45
O21b–ZrO	88.98	O21a–Zr–Cl	101.12
O21b–Zr–Cl	101.42	O23a–ZrO	81.82
O21a–Zr–O23a	84.11	O–Zr–Cl	102.78
O23b–Zr–O23a	78.23	O23b–Zr–Cl	97.89
Charges			
Zr	0.988	O	0.154
O23a	−0.385	Cl	−0.297
O21a	−0.388	O23b	−0.354
O22a	−0.421	O21b	−0.399
O22b	−0.416		
Total energy/au	−492.57021		
Total dipole moment/D	10.69		

one $O_{carboxylate}$ atom of each ciprofloxacin ligand and Cl ion. The Zr–O21a and Zr–O21b bond lengths are 2.192 and 2.194 Å, respectively, are shorter than that of Zr–O23a and Zr–O23b (2.404 and 2.195 Å, respectively) and the bond distance between Zr–Cl is 2.299 Å [53]. Also the angles around the central Zr(IV) metal ion with surrounding oxygen atoms vary from 73.053 to 101.42; these values agree with these expected for a distorted octahedron.

The charges accumulated on $O_{carboxylate}$ are −0.388 and −0.399 and for O_{keto} are −0.385 and −0.354 in chloride complex while for water complex the charges on $O_{carboxylate}$ are −0.367 and −0.372 and O_{keto} is −0.335 and −0.376, so that the Zr(IV) metal ion is bonded strongly with surrounded oxygen atoms of ciprofloxacin in chloride complex more than that in water complex. There is a strong interaction between central Zr(IV) metal ion which become has charge equal +0.988 in chloride complex. The energy of this complex is −492.57021 au and highly dipole 10.69 D. For all these reasons the chloride complex is more stable than water complex and Zr(IV) favor coordinated with one ion of chloride more than one molecule of water to complete the octahedron structure.

References

[1] D.C. Hooper, J.S. Wolfson, Quinolone Antimicrobial Agent, second ed., American Society of Microbiology, Washington, DC, U.S.A., 1995.
[2] G. Pasomas, J. Inorg. Biochem. 102 (2008) 1798.
[3] D.E. King, R. Malone, S.H. Lilley, Am. Fam. Phys. 61 (2000) 2741.
[4] P. Drevenšek, N.P. Ulrih, A. Majerle, I. Turel, J. Inorg. Biochem. 100 (2006) 1705.
[5] I. Turel, Coord. Chem. Rev. 232 (2002) 27.
[6] E.K. Efthimiadou, Y. Sanakis, C.P. Raptopoulou, A. Karaliota, A. Katsaros, G. Pasomas, Bioorg. Med. Lett. 16 (2006) 3864.
[7] E.K. Efthimiadou, A. Karaliota, G. Pasomas, Polyhedron 27 (2008) 349.
[8] K. Shiba, M. Sakamoto, Y. Nakazawwa, O. Sakai, Fifth International Symposium on New Quinolones (Programme and Abstract), 95, 1994.
[9] I. Turel, K. Gruber, I. Leban, N. Bukovec, J. Inorg. Biochem. 61 (1996) 197.
[10] Z.F. Chen, R.J. Xiong, J.L. Zuo, Z. Guo, X.Z. You, K.H. Fun, J. Chem. Soc. Dalton Trans. 22 (2000) 4013.
[11] I. Turel, L. Leban, G. Klintschar, N. Bukovec, S. Zalar, J. Inorg. Biochem. 66 (1997) 77.
[12] M. Ruiz, R. Ortiz, L. Perello, J.S. Carrio, J. Inorg. Biochem. 65 (1997) 87.
[13] M. Ruiz, L. Perello, R. Ortiz, A. Castineiras, C.M. Mossmer, E. Canton, J. Inorg. Biochem. 59 (1995) 801.
[14] B. Macias, M.V. Villa, I. Rubio, A. Castineiras, J. Borras, J. Inorg. Biochem. 84 (2001) 163.
[15] K.C. Skyrianou, E.K. Efthimiadou, V. Psycharis, A. Terzis, D.P. Kessissoglou, G. Pasomas, J. Inorg. Biochem. 104 (2009) 1617.
[16] Gaussian 98, Revision A.6, M. J. Frisch, G. W. Trucks, H. B. Schlegel, G. E. Scuseria, M. A. Robb, J. R. Cheeseman, V. G. Zakrzewski, J. A. Montgomery, Jr., R. E. Stratmann, J. C. Burant, S. Dapprich, J. M.Millam, A. D. Daniels, K. N. Kudin, M. C. Strain, O. Farkas, J. Tomasi, V. Barone, M. Cossi, R. Cammi, B. Mennucci, C. Pomelli, C. Adamo, S.Clifford, J. Ochterski, G. A. Petersson, P. Y. Ayala, Q. Cui, K. Morokuma, D. K. Malick, A. D. Rabuck, K. Raghavachari, J. B. Foresman, J.Cioslowski, J. V. Ortiz, B. B. Stefanov, G. Liu, A. Liashenko, P. Piskorz, I. Komaromi, R. Gomperts, R. L. Martin, D. J. Fox, T. Keith, M. A. Al-Laham, C. Y. Peng, A. Nanayakkara, C. Gonzalez, M. Challacombe, P. M. W. Gill, B. Johnson, W. Chen, M. W. Wong, J. L.Andres, C. Gonzalez, M. Head-Gordon, E. S. Replogle, and J. A. Pople, Gaussian, Inc., Pittsburgh PA, 1998.
[17] W.J. Stevens, M. Krauss, H. Bosch, P.G. Jasien, Can. J. Chem. 70 (1992) 612.
[18] S.A. Sadeek, J. Mol. Struct. 753 (2005) 1.
[19] S.A. Sadeek, M.S. Refat, H.A. Hashem, J. Coord. Chem. 59 (2006) 7.
[20] S.A. Sadeek, W.H. EL-Shwiniy, J. Mol. Struct. 977 (2010) 243.
[21] S.A. Sadeek, W.H. EL-Shwiniy, J. Mol. Struct. 981 (2010) 130.
[22] S.A. Sadeek, W.H. EL-Shwiniy, J. Coord. Chem. 63 (2010) 3471.
[23] S.A. Sadeek, W.H. EL-Shwiniy, W.A. Zordok, A.M. EL-Didamony, J. Argent. Chem. Soc. 97 (2009) 128.
[24] S.A. Sadeek, A.M. EL-Didamony, W.H. EL-Shwiniy, W.A. Zordok, J. Argent. Chem. Soc. 97 (2009) 51.
[25] D.J. Beecher, A.C. Wong, Identification of hemolysin Bl-producing *Bacillus cereus* isolated by a discontinuous hemolytic pattern in blood agar, Appl. Environ. Microbiol. (1994).
[26] W.J. Geary, Coord. Chem. Rev. 7 (1971) 81.
[27] R.M. Silverstein, G.C. Bassler, T.C. Morril, Spectroscopic Identification of Organic Compounds, fifth ed., Wiley, New York, 1991.
[28] F. Gao, P. Yang, J. Xie, H. Wang, J. Inorg. Biochem. 60 (1995) 61.
[29] I. Turel, P. Bukovec, M. Quiros, Int. J. Pharm. 152 (1997) 59.
[30] K. Nakamoto, Infrared and Raman Spectra of Inorganic and Coordination Compounds, fourth ed., Wiley, New York, 1986.
[31] M.S. Refat, Spectrochim. Acta 68 (2007) 1393.
[32] G. Pasomas, A. Tarushi, E.K. Efthimiadou, Polyhedron 27 (2008) 133.
[33] F.A. Cotton, G. Wilkinson, C.A. Murillo, M. Bochmann, Advanced Inorganic Chemistry, sixth ed., Wiley, New York, 1999.
[34] F.A. Cotton, C.W. Wilkinson, Advanced Inorganic Chemistry, Third ed., Interscience Publisher, New York, 1972.
[35] A.W. Coats, J.P. Redfern, Nature 201 (1964) 68.
[36] H.W. Horowitz, G. Metzger, Anal. Chem. 35 (1963) 1464.
[37] I. Muhammad, I. Javed, I. Shahid, I. Nazia, Turk. J. Biol. 31 (2007) 67.
[38] T. Skauge, I. Turel, E. Sletten, Inorg. Chim. Acta 339 (2002) 239.
[39] M.N. Hughes, The Inorganic Chemistry of Biological Processes, second ed., Wiley, New York, 1981.
[40] M. Imran, J. Iqbal, S. Iqbal, N. Ijaz, Turk. J. Biol. 31 (2007) 67.
[41] E.K. Efthimiadou, A. Karaliota, G. Pasomas, J. Inorg. Biochem. 104 (2010) 455.
[42] W. Kohn, L.J. Sham, Phys. Rev. A 140 (1965) 1133.
[43] A.D. Becke, Phys. Rev. A 38 (1988) 3098.
[44] C. Lee, W. Yang, R.G. Parr, Phys. Rev. B 37 (1988).
[45] R.L. Flurry Jr., Molecular Orbital Theory of Bonding in Organic Molecules, Marcel Decker, New York, 1968.
[46] I. Turel, I. Leban, N. Bukovec, J. Inorg. Biochem. 66 (1997) 241.
[47] I. Turel, L. Golic, P. Bukovec, M. Gubina, J. Inorg. Biochem. 71 (1998) 53.
[48] R. Khoshnavazi, A. Salimi, A. Ghiasi Moaser, Polyhedron 27 (2008) 1303.
[49] L.L. Shen, in: D.C. Hopper, J.S. Wolfson (Eds.), Quinolone Antimicrobial Agents, second ed., American Sociaty for Microbiology, Washington, DC, 1993.
[50] P.C. Andrews, T. Beck, B.H. Frasr, P.C. Junk, M. Massi, Polyhedron 26 (2007) 5406.
[51] Q. Chen, Y.D. Chang, J. Zubieta, Inorg. Chem. Acta 258 (1997) 257.
[52] G. Paolucci, M. Vignola, L. Coletto, B. Pitteri, F. Benetollo, J. Organ. Chem. 687 (2003) 161.
[53] A. Antinolo, R. Fernandez-Galan, A. Otero, S. Prashar, I. Rivilla, A.M. Rodriguez, J. Organ. Chem. 691 (2006) 2924.
[54] T. Cuenca, P. Gomez-Sal, C. Martin, B. Royo, P. Royo, J. Organ. Chem. 588 (1999) 134.
[55] D.P. Steinhuebel, P. Fuhrmann, S.J. Lippard, Inorg. Chem. Acta 270 (1998) 527.
[56] W. Petz, F. Weller, E.V. Avtomonov, J. Organ. Chem. 598 (2000) 403.